Double Jet Emission of Hot Electrons from a Micro-droplet Spray

You may also be interested in:

Effects of Polarization on Super-hot Electron Generation inFemtosecond Laser-Plasma Interaction
Zhang Ping, Liang Tian-Jiao, Chen Li-Ming et al.

Simulation for Interaction of Linearly Polarized RelativisticLaser Pulses with Foil Targets
Liu Shi-Bing, Tu Qin-Fen, Yu
Wei et al.

The dissociative ionization and Coulomb explosion of ethane by a femtosecond laser field
Li Xia, Ren Hai-Zhen, Ma Ri et al.

Ion Acceleration by an Electrostatic Field in the InteractionBetween Femtosecond Laser Pulses and
Solid Targets
Dong Quan-Li, Zhang Jie, Liang Tian-Jiao et al.

Investigation on laser–plasma coupling in intense, ultrashort irradiation of a nanostructured
silicon target
G Cristoforetti, A Anzalone, F Baffigi et al.

Generation of Helical and Axial Magnetic Fields by theRelativistic Laser Pulses in Under-dense
Plasma: Three-DimensionalParticle-in-Cell Simulation
Zheng Chun-Yang, Zhu Shao-Ping and He
Xian-Tu

Double Jet Emission of Hot Electrons from a Micro-droplet Spray *

PENG Xiao-Yu(彭晓昱)[1], ZHANG Jie(张杰)[1,**], LIANG Tian-Jiao(梁天骄)[1,2], SHENG Zheng-Ming(盛政明)[1],
JIN Zhan(金展)[1], LI Yu-Tong(李玉同)[1], WANG Zhao-Hua(王兆华)[1], YU Quan-Zhi(于全芝)[1],
ZHENG Zhi-Yuan(郑志远)[1], LIU Yun-Quan(刘运全)[1], WU Hui-Chun(武慧春)[1], HAO Zuo-Qiang(郝作强)[1],
YUAN Xiao-Hui(远晓辉)[1], WEI Zhi-Yi(魏志义)[1]

[1]*Laboratory of Optical Physics, Institute of Physics, Chinese Academy of Sciences, Beijing 100080*
[2]*Research Institute of Chemical Defenses, Beijing 102205*

(Received 29 December 2003)

Spatial distribution of hot electrons with energies above 50 keV are investigated by an ethanol micro-droplet spray irradiated by linearly and elliptically polarized 150 fs laser pulses at an intensity of 10^{16} W/cm^2. Two symmetric hot electron jets with respect to the laser propagation direction are observed in the polarization plane for a linearly polarized laser field and in the plane of the long electric vector for an elliptically polarized laser field, respectively. Particle-in-cell simulations suggest that the resonance absorption on the spherical surface of the droplets is mainly responsible for the generation of the double-jet emission of hot electrons.

The interaction of intense laser pulses with solid[1−3] and cluster targets[4−6] has been widely studied since the development of ultrashort-pulsed high intensity lasers, based on the chirped pulse amplification (CPA) technique.[7] Researchers[8−11] have investigated the angular distribution of energetic electrons in laser–solid and laser–cluster interactions. It is important to study the distribution of hot electrons to understand the mechanism of laser–plasma interaction, the spatial distributions of the ions, x- and γ-rays, and the visible lights from plasmas. Recently, micro-droplets, a new kind of target between solid and cluster targets with very limited mass and micron-scale size, have aroused broad interest.[12−14] In this Letter, we report the measurements of spatial distribution of hot electrons in 2π space from ethanol droplets irradiated by linearly and elliptically polarized laser pulses with duration of 150 fs at an intensity of 10^{16} W/cm^2. The results indicate that the spatial distribution of hot electrons strongly depends on the polarization state of the laser field.

The experiments were carried out in our laboratory with a Ti:sapphire chirped pulse amplification (CPA) laser system operated at around 800 nm at a repetition rate of 10 Hz. Figure 1 shows the schematic experimental setup. The laser delivered 5-mJ energy in 150-fs pulses with a peak-to-pedestal contrast ratio of 10^5 at about 20 ps before the peak. A laser beam was focused with an 80-mm focal length lens, yielding a peak intensity of 10^{16} W/cm^2 at a focus with a diameter of about $20\,\mu$m. The laser polarization is changed by rotating a half-wave plate and a quarter-wave plate to investigate the dependence on polarization. A solenoid-driven pulsed valve with a 100-μm orifice was used to generate ethanol droplets.

The valve was pulsed for 460-μs duration at a repetition rate of 10 Hz. High-pressure nitrogen gas along the gas line propelled ethanol in the liquid reservoir to stream through the orifice. Thus high-density polydisperse sprays containing several-micron-scale ethanol droplets were formed in vacuum. The droplet size was measured using an optical imaging system. The droplet spray with a subsonic velocity out from the 100-μm diameter orifice was back-illuminated with frequency-doubled light (400 nm, 150 fs) of the main laser beam and their shadows were magnified and imaged to a charge coupled device (CCD) camera. The spatial resolution of the imaging system was approximately $2.0\,\mu$m. The mean droplet diameter is $4\,\mu$m. The number density of the spray, N, can be determined by measuring the rate at which liquid flows through the orifice and is dispersed into a given volume.[15] In our experiments, the mean number density of the spray at 1mm from the orifice is about 5.4×10^8 droplets/cm^3.

The main laser beam was focused in the central region of the droplet spray under the orifice (as shown in Fig. 1). The focusing condition at the centre of the spray was monitored using a γ-ray spectrometer and a calorimeter. X-ray Bremsstrahlung radiation from the laser plasma can be monitored simultaneously.

Spatial distributions of hot electron emission were measured with an array of LiF thermoluminescent dosimeter (TLD) pieces attached inside a hemisphere shell. The TLD detectors were wrapped with a 20-μm-thick aluminium foil, which can block energetic ions, scattered laser lights, soft x-rays, and electrons with energies below 50 keV. The energetic hard x-rays can pass through the Al foil and the TLDs. Thus, hot electrons with energies over 50 keV mainly contributed to

the dosage recorded by the TLDs. The centre of the hemisphere was at the laser focus and the equatorial plane was placed parallel to the horizontal plane. The angular resolution of this system was better than 10°.
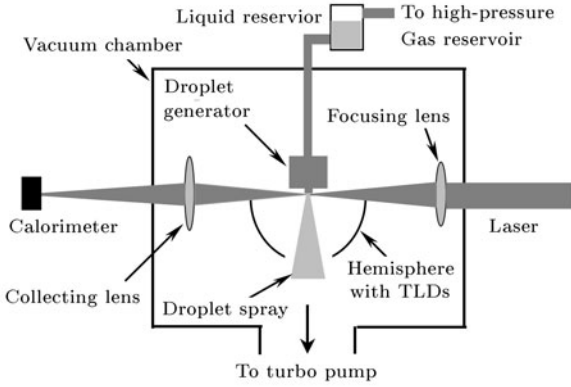

Fig. 1. Schematic of experimental setup for measurements of the spatial distribution of hot electrons from laser–droplet interactions.

The spatial distributions for hot electrons from the droplet spray are shown in Fig. 2. The figures on the left are the sketch maps for three different polarizations of the laser field. The dose was accumulated over 18000 shots. In order to make a comparison, the doses shown in Figs. 2(a)–(c) were normalized to the maximum of themselves respectively. Figure 2(a) shows the spatial distribution of hot electrons when the polarization plane of the linearly polarized laser beam is coincident with the equatorial plane of the hemisphere (or the horizontal plane). From Fig. 2(a) one can find that the hot electrons mainly distribute among the front-hemisphere of the detector. The distinct feature is that a double jet emission of hot electrons was found to be symmetric with respect to the laser propagation direction in the polarization plane. The angles corresponding to the strongest emission with respect to the laser axis in the polarization plane are around ±60°. When the plane of the laser polarization was rotated about 60° by rotating the half-wave plate, the hot electron jet was found to rotate about 60° accordingly, shown in Fig. 2(b). The other jet cannot be seen because it cannot be recorded by the detectors of the hemisphere. This result indicates that hot electrons only emit in the laser polarization plane. To validate further this conclusion, an elliptically polarized laser beam (with a polarization ratio of about 50%) with its plane of the longer electric vector coincident with the equatorial plane of the hemisphere by rotating a quarter-wave plate was used to irradiate the droplet spray in Fig. 2(c). Two symmetric hot electron jets with respect to the laser propagation direction were also observed in the plane of the long electric vector in the elliptically polarized laser field. However, the spatial distribution of hot electron emission is not so concentrated, as seen in Fig. 2(a). This is due to the fact that there are different components of the

electric vectors in the elliptically polarized laser field and all these components irradiate the front surface of the droplets. Although the hot electrons mainly distribute in the front-hemisphere, forward emission of hot electrons can also be observed to be much weaker than the anterior ones from Fig. 2. This indicates that not only ejecting hot electrons but also injecting ones can be generated from the laser–droplet interaction. The injecting electrons are absorbed and attenuated by the target droplets themselves. All the results in Fig. 2 show that the spatial distributions of hot electrons strongly depend on the laser polarization state. The above results are similar to those of in Ref. [16], where the laser beam was focused on the surface of bulk water in air.

We find that even though the solid angle of the emission of the hot electrons is symmetric with respect to the laser axis, the intensities of the two jets of hot electrons are not identical. This is because the main laser beam was not focused well or not exactly focused in the central region of the droplet spray. This indicates that the attenuation and the absorption of a mass of droplets around the focus spot would affect the pattern of spatial distributions of hot electrons to some extent. The above speculation was confirmed in further measurements by only changing the focusing position deliberately under the same experimental conditions. However, the movement of the focusing position only changes the angular distributions on the equatorial plane, but does not affect the above result.

Collimated hot electron emission can be generated by different acceleration mechanisms, such as resonance absorption,[17] vacuum heating,[18] abnormal skin effects,[19] and pondermotive $\boldsymbol{J} \times \boldsymbol{B}$ heating.[20] However, only resonance absorption and vacuum heating have oblique-incidence effects and depend strongly on the polarization state of the laser beam, because of the unique geometry of droplets, and whether or not the linearly polarized laser or the elliptically polarized laser has a component of the electric field along the direction of the density gradient as it irradiates on the spherical droplet surface. For a spherical surface, the laser incident angle changes from 0° to ±90° if we only consider the droplets within the Rayleigh volume of the focus. This means that the majority of laser light obliquely irradiates on the droplet surface. Furthermore, the above experimental results indicate that the hot electron distribution strongly depends on the laser polarization state. Therefore, we speculate that the resonance absorption and the vacuum heating might be mainly responsible for the generation of hot electrons in our experiments.

To explain the experimental results, we ran a two-dimensional particle-in-cell (PIC) simulation with different density scale length $L = (\partial \ln n_e/\partial z)^{-1}$ and electron density n_e. The spherical droplets are approximated as infinitely long cylinders with a diameter of $4 \,\mu$m. The simulation box size is $25\,\lambda \times 30\,\lambda$. This
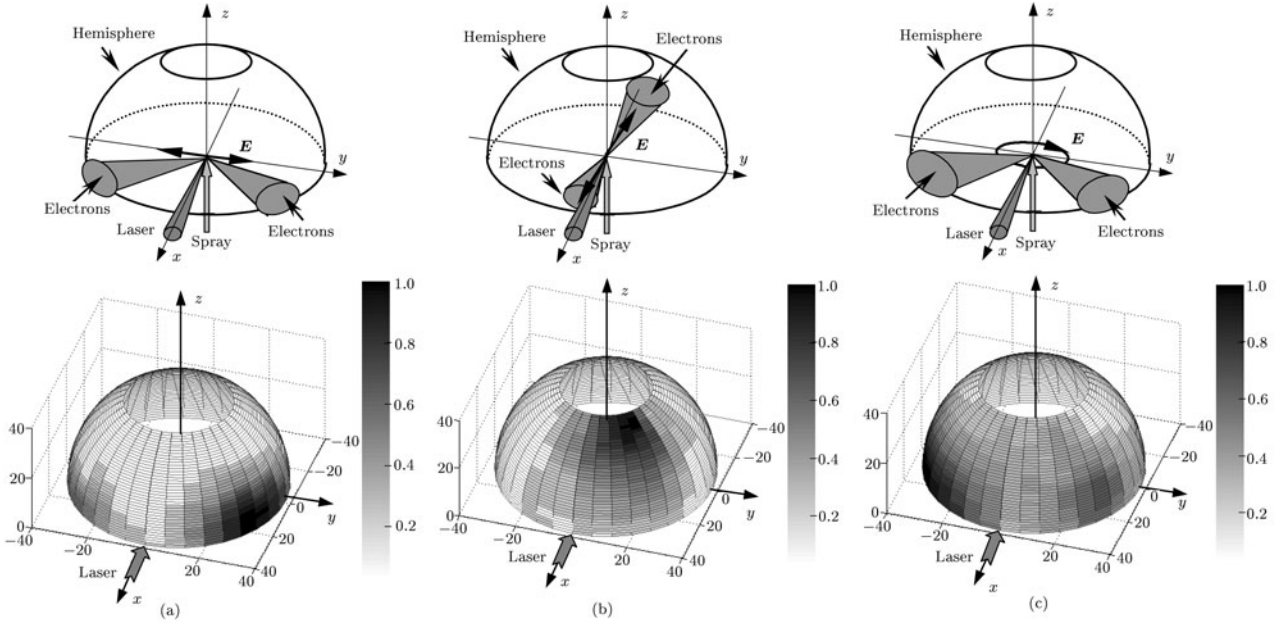
Fig. 2. Characteristics of 2π spatial distribution of the hot electrons with energies over $50\,\mathrm{keV}$ from ethanol droplet spray irradiated by laser pulses linearly polarized in the horizontal plane (a) and at about $60°$ with respect to horizontal plane (b), and by elliptically polarized laser pulses (c). The electric vectors of the laser beam are shown on the left. The laser intensity is $10^{16}\,\mathrm{W/cm^2}$. Double jet emission of hot electrons strongly depends on the laser polarization state.
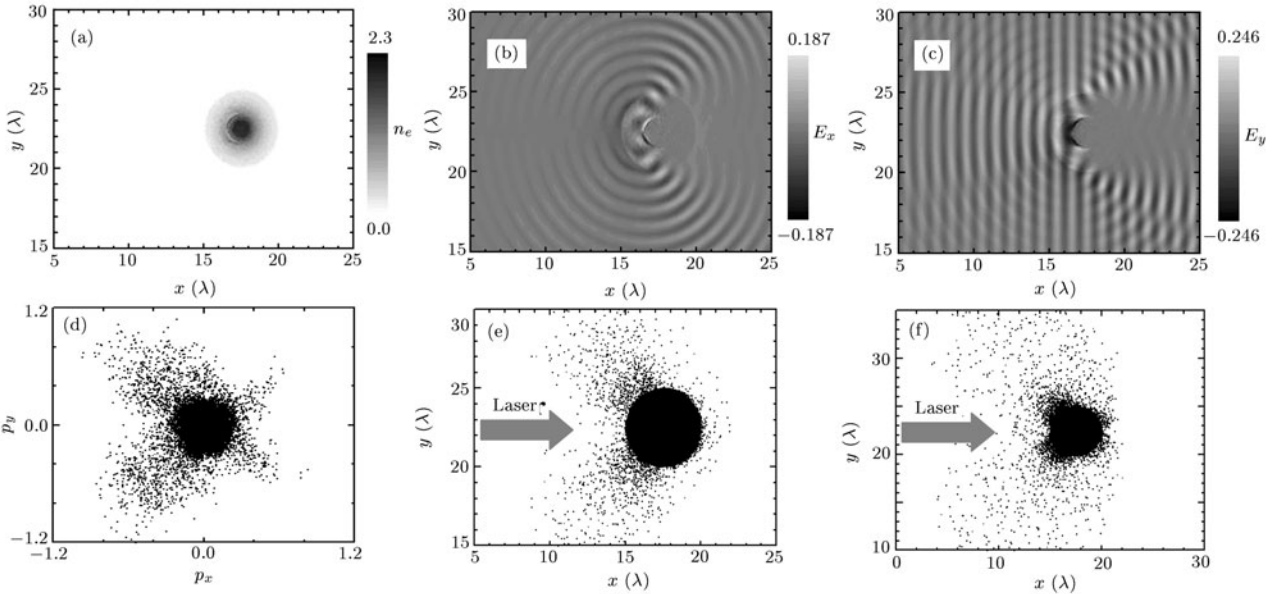

Fig. 3. Two-dimensional PIC simulation results for a micro-droplet irradiated by linearly polarized laser pulses with polarization plane parallel to the horizontal plane at the 50th laser cycle (a)–(e), and at the 60th laser cycle (f). (a), Electron density profile; (b), the longitudinal component of the resonantly excited electric field; (c), the transverse component of the resonantly excited electric field; (d), p_y versus p_x; (e) and (f), distributions of electrons on the $x\,y$ plane at the 50th and 60th laser cycles, respectively.

droplet-plasma is irradiated by a linearly polarized laser pulse with its polarization plane parallel to the horizontal plane. Provided that $a_0 = 0.1$, corresponding to the laser intensity at focus slightly larger than $10^{16}\,\mathrm{W/cm^2}$, the laser pulse is incident from left normally on to the droplet-plasma. We find that in the case of abrupt electron density gradient, which is suitable for vacuum heating, no distinct strong directional

emission of hot electrons can be observed, while only a nearly isotropic distribution of electrons can be observed. If we take the electron density L increasing from $0.2\,n_c$ exponentially with a scale length of $0.9\,\lambda$ until about $2.0\,n_c$, where n_c is the critical density, we find that the simulations can best reproduce our main experimental results. Figure 3 shows the simulation results at the 50 laser cycles. Initially, we find that the

electron density near the critical surface changes and both the longitudinal and transverse components of the excited electric field on the frontal surface become stronger with time elapsing. At about the 50th laser cycle, $\nabla n/n$ near the critical surface reaches the maximum, and the maximum electron density is $2.3\,n_c$, as shown in Fig. 3(a). At this time the longitudinal and the transverse electric fields around the critical surface reach their maxima that are much stronger than the initial laser electric field. Figures 3(b) and (c) depict the longitudinal and transverse components of the resonantly excited electric field at the 50th laser cycle, respectively. It is the enhanced oscillating electric field around the critical density surface that accelerates the electrons to high energies. Figure 3(d) ex-

hibits the behaviour of p_y versus p_x at the 50th laser cycle. We can find that electron jets goes out from the droplet surface until the 40th laser cycle. At the 50th laser cycle, it is very obvious that two groups of the collimated electrons are accelerated to high energies symmetrically with respect to the laser axis from the spatial distribution ($x-y$ plot) of the electrons in Fig. 3(e). At the 60th laser cycle, lateral electrons can be observed from Fig. 3(f). In the entire course, the strong emission is in the range from about $\pm40°$ to about $\pm80°$. This agrees well with the spatial distribution of hot electrons measured in our experiments. Our simulation suggests that the resonance absorption is mainly responsible for the generation of the double jet of hot electrons.
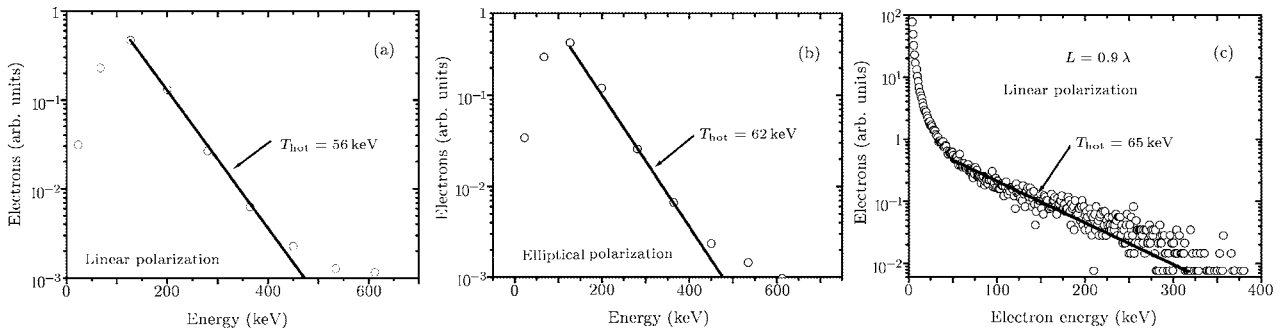

Fig. 4. Hot electron energy spectra from the ethanol droplets irradiated by linearly polarized laser pulses (a) and by elliptically polarized laser pulses (b). The experimental conditions are the same as those in Figs. 2(a) and (c), respectively, with a magnetic spectrometer placed in the direction of about $50°$ with respect to the laser axis on the equatorial plane. (c) The time-integrated hot electron spectrum of ethanol droplets with density scale length $L = 0.9\lambda$ after 80 optical cycle from the PIC simulation.

To validate further the above conclusion, we also directly measured the energy spectrums of the hot electrons with a magnetic spectrometer under the same conditions as those in Figs. 2(a) and (c). Figures 4(a) and (b) show the results from the ethanol droplet spray irradiated by linearly and elliptically polarized laser pulses, respectively. Figure 4(c) shows the result from the PIC simulation. The temperature of the resonantly heated electrons from the simulation is 65 keV, which is very similar to our experimental results of 56 keV and 62 keV.

In conclusion, we suggest that the resonance absorption is the main mechanism for the generation of the double jet emission of hot electrons in our experiments. The measurements also indicate that we can get any directional jets of hot electrons from a microdroplet spray by changing the laser polarization direction.

References

[1] Davies J R et al 1997 *Phys. Rev.* E **56** 7193
[2] Yu W et al 2000 *Phys. Rev. Lett.* **85** 570
[3] Tao Y Z et al 2002 *Chin. Phys. Lett.* **19** 956
[4] Ditmir T et al 1995 *Phys. Rev. Lett.* **75** 3122
[5] Ditmir T et al 1997 *Nature* **386** 54
[6] Li S H et al 2003 *Chin. Phys. Lett.* **20** 1247
[7] Strickland D and Mourou G 1985 *Opt. Commun.* **56** 219
[8] Sheng Z M et al 2000 *Phys. Rev. Lett.* **85** 5340
[9] Chen L M et al 2002 *Phys. Rev.* E **66** 025402R
[10] Sentoku Y, Ruhl H, Mima K, Kodama R, Tanaka K A and Kishimoto Y 1999 *Phys. Plasmas* **6** 2855
[11] Chen L M, Zhang J, Li Y T, Teng H, Liang T J, Sheng Z M, Dong Q L, Zhao L Z, Wei Z Y and Tang X W 2001 *Phys. Rev. Lett.* **87** 225001
[12] Gumbrell E T, Comley A J, Hutchinson M H R and Smith R A 2001 *Phys. Plasmas* **8** 1329
[13] Mcnaught S J, Fan J, Parra E and Milchberg H M 2001 *Appl. Phys. Lett.* **79** 4100
[14] Favre C, Boutou V, Hill S C, Zimmer W, Krenz M, Lambrecht H, Yu J, Chang R K, Woeste L and Wolf J P 2002 *Phys. Rev. Lett.* **89** 035002
[15] Mountford L C, Smith R A and Hutchinson M H R 1998 *Rev. Sci. Instrum.* **69** 3780
[16] Li Y T, Zhang J, Sheng Z M, Teng H, Liang T J, Peng X Y, Lu X, Li Y J and Tang X W 2003 *Phys. Rev. Lett.* **90** 165002
[17] Estabrook K and Kruer W L 1978 *Phys. Rev. Lett.* **40** 42
[18] Brunel F 1987 *Phys. Rev. Lett.* **59** 52
[19] Wilks S C, Kruer W L, Tabak M and Langdon A B 1996 *Phys. Rev. Lett.* **69** 1383
[20] Malka G, Fuchs J, Amiranoff F, Baton S D, Gaillard R, Miquel J L, Pépin H, Rousseaux C, Bonnaud G, Busquet M and Lours L 1997 *Phys. Rev. Lett.* **79** 2053